CHAPTER 26

Computational Methods for Biomolecular Electrostatics

Feng Dong, Brett Olsen, and Nathan A. Baker

Department of Biochemistry and Molecular Biophysics
Center for Computational Biology
Washington University in St. Louis, Missouri 63110

Abstract

An understanding of intermolecular interactions is essential for insight into how cells develop, operate, communicate, and control their activities. Such interactions include several components: contributions from linear, angular, and torsional

METHODS IN CELL BIOLOGY, VOL. 84

0091-679X/08 $35.00
DOI: 10.1016/S0091-679X(07)84026-X

forces in covalent bonds, van der waals forces, as well as electrostatics. Among the various components of molecular interactions, electrostatics are of special importance because of their long range and their influence on polar or charged molecules, including water, aqueous ions, and amino or nucleic acids, which are some of the primary components of living systems. Electrostatics, therefore, play important roles in determining the structure, motion, and function of a wide range of biological molecules. This chapter presents a brief overview of electrostatic interactions in cellular systems, with a particular focus on how computational tools can be used to investigate these types of interactions.

I. Introduction

Intermolecular interactions are essential for nearly every cellular activity. The forces that underlie these interactions include van der Waals dispersion and repulsion, hydrogen bonding, and electrostatics. Electrostatic forces are especially important in biological systems because most biomolecules are charged or polar. For example, nucleic acids contain long strings of negative charges while proteins are generally zwitterionic with a wide variety of amino acids that make up a complex charge distribution. Even the solvent environment in which the larger molecules interact is full of polar water and an assortment of simple ions. Therefore, insight into the most fundamental biomolecular processes requires a basic understanding of electrostatics. This chapter first presents a brief overview of electrostatics in biological systems, followed by a discussion of several different models that can simplify the analysis of electrostatics, and concludes with specific applications of computational electrostatics models for biological systems.

II. Electrostatics in Cellular Systems

Electrostatic interactions are ubiquitous for any system of charged or polar molecules, such as biomolecules in their aqueous environment. For example, proteins are made up of 20 types of amino acids, 11 of which are charged or polar in neutral solution. Nucleic acids contain long stretches of negative charges from the phosphate groups in nucleotides. Finally, sugars and related glycosaminoglycans can possess some of the highest charge densities of any biomolecules because of the presence of numerous negative functionalities, including carboxylate and sulfate groups. We will focus on a few specific examples of electrostatic interactions in cellular systems: biomolecule–ion, biomolecule–ligand, and biomolecule–biomolecule interactions. Each of these interactions will be discussed in more detail in the following sections.

A. Biomolecule–Ion Interactions

In cellular settings, biomolecules are immersed in solution along with water, ions, and numerous other small molecules and macromolecules. Ions influence biomolecular processes and interactions in several different ways, including long-range screening, site-specific ion binding, and preferential hydration effects. Long-range screening is a phenomenon in which the strength of electrostatic interactions within and between biomolecules is reduced by the presence of aqueous ions. This is a nonspecific ion effect and is described well, at low salt charge and concentration, by the Debye–Hückel theory (Debye and Hückel, 1923) and the related implicit solvent models described in Section III.B. In site-specific ion binding, ions interact with biomolecules by binding to specific sites in a manner similar to ligand binding (see Section II.B; Draper *et al.*, 2005). Preferential hydration or Hofmeister effects are species-specific competitions between ions and water for binding to nonspecific sites on biomolecules (Boström *et al.*, 2006; Collins, 2006; Hofmeister, 1888). This competition is between weak biomolecule–solvent and biomolecule–ion interactions and therefore observed only at very high salt concentrations (Anderson and Record, 2004; Eisenberg, 1976). A similar effect involves competition between ionic species around charged biomolecules (Moore and Lohman, 1994; Reuter *et al.*, 2005). Note that, although these effects can be important, preferential hydration and ion–ion competition are not routinely considered in simulations, mainly because of limitations in current computational methodology. While there is active work in improving the theoretical and computational treatment of these effects (Boström *et al.*, 2003, 2006; Broering and Bommarius, 2005; Shimizu, 2004; Shimizu and Smith, 2004; Zhou, 2005), they are currently beyond the scope of this chapter.

Ion-induced RNA folding (Cech and Bass, 1986; Dahm and Uhlenbeck, 1991; Draper *et al.*, 2005; Misra and Draper, 2000, 2001; Römer and Hach, 1975; Stein and Crothers, 1976) provides an excellent example of many of the ion–biomolecule interactions discussed above. RNA folding in the absence of salt is quite unfavorable due to a number of negative charges along its phosphodiester backbone. Bringing these negative charges together into a compact structure introduces a large energetic barrier to RNA folding. Positive ions promote folding by reducing the repulsion between these negative charges. However, some ions are more effective than others; for example, millimolar concentrations of Mg^{2+}can stabilize RNA tertiary structures that are only marginally stable in solution with a high concentration of monovalent cations, such as Na^{+}or K^{+}(Cole *et al.*, 1972; Romer and Hach, 1975; Stein and Crothers, 1976). Accurately modeling the ion–RNA interactions is essential to explain this phenomenon. A major obstacle in modeling ion–RNA interactions is the presence of numerous different ion environments (Draper *et al.*, 2005). Each environment is dominated by different types of ion–biomolecule interactions described above and requires different approaches to evaluating the energies. For example, experimental results for Mg^{2+}effects on $tRNA^{Phe}$ folding can be modeled successfully while only considering long-range

screening effects (Misra and Draper, 2000). However, the diffusive Mg^{2+} ion description provided by this model is not sufficient to describe the folding of a 58-nt rRNA fragment. Instead, one Mg^{2+} ion must be explicitly included at a specific binding site (Misra and Draper, 2001). A comprehensive theoretical framework of ion–RNA interactions that accounts for the overall ion dependence of RNA folding is the aim of current RNA folding studies (Draper *et al.*, 2005).

B. Biomolecule–Ligand and –Biomolecule Interactions

Biomolecule–substrate recognition is central to nearly all biomolecular processes, including signal transduction, enzyme cooperativity, and metabolic regulation. The bimolecular binding process, from a kinetic perspective, can be reduced to two steps: diffusional association to form an initial encounter complex and nondiffusional rearrangement to form the fully bound complex. The diffusional association places an upper limit on the overall binding rate; so-called ''perfect'' enzymes operate at this diffusion-limited rate. Electrostatic forces have an important influence on biomolecular diffusional association: their long-range nature enables them to attract the substrate to its binding partner and orient the substrate properly for binding (Gabdoulline and Wade, 2002). It has been established that for many biomolecular complexes, electrostatic interactions can significantly affect bimolecular association rates (Law *et al.*, 2006). For example, by using Brownian dynamics (BD) simulations (Ermak and McCammon, 1978; Northrup *et al.*, 1984; Section IV.F) to calculate diffusional association rates, Gabdoulline and Wade demonstrated that for fast-associating protein pairs, electrostatic interactions enhance association and are the dominant forces determining the rate of diffusional association (Gabdoulline and Wade, 2001; Radic *et al.*, 1997). Using related methods, Sept *et al.* demonstrated the role of electrostatic interactions in determining the rates and polarity of actin polymerization (Sept and McCammon, 2001; Sept *et al.*, 1999).

Electrostatic interactions also play an important role in determining the thermodynamics of binding, that is, binding affinity (Chong *et al.*, 1998; Norel *et al.*, 2001; Novotny and Sharp, 1992; Rauch *et al.*, 2002; Schreiber and Fersht, 1993, 1995; Sheinerman *et al.*, 2000; Zhu and Karlin, 1996). Substrate binding allows the formation of (potentially) favorable charge–charge interactions between the substrate and the target, as well as stabilizing specific salt bridges and hydrogen bonds (Chong *et al.*, 1998; Schreiber and Fersht, 1993, 1995). However, at the same time, charges on the molecular binding surface must shed their bound water in order to allow close binding. This loss of water, or desolvation, is generally energetically unfavorable and offsets the favorable interactions formed on binding. The binding affinities, from an electrostatic point of view, are determined by the balance of these two energetic contributions (del Álamo and Mateu, 2005; Lee and Tidor, 2001; Russell *et al.*, 2004; Sheinerman and Honig, 2002; Xu *et al.*, 1997). Systematic studies of protein pairs, such as barnase and barstar (Dong *et al.*, 2003; Frisch *et al.*, 1997; Schreiber and Fersht, 1993, 1995), and fasciculin-2

(Radic *et al.*, 1997), as well as protein kinase A and balanol (Wong *et al.*, 2001), have shown that charged and polar residues at the protein–protein interfaces play important roles in binding energetics. Similarly, Sept *et al.* (2003) have demonstrated an important role for electrostatics in determining microtubule structure and stability. Finally, Wang *et al.* (2004) have demonstrated that nonspecific electrostatic interactions can provide a driving force for recruitment of proteins to intracellular membranes, an important step in signal transduction.

However, despite the role of electrostatics in protein–protein interactions, it is important to realize that the total interaction is also strongly influenced by shape complementarity at the protein–protein interface as well as by nonpolar contributions to offset the penalties of desolvation (Janin and Chothia, 1990; Lo Conte *et al.*, 1999; Ma *et al.*, 2003; Vasker, 2004).

III. Models for Biomolecular Solvation and Electrostatics

As described above, computer simulations can provide atomic-scale information on energetic and dynamic contributions to biomolecular structure and interactions. However, the capabilities of computer simulations are limited by the accuracy of the underlying models describing atomic interactions and also by the computational expense of adequately exploring all the relevant conformations of the biomolecule and surrounding water and ion. Therefore, most models of biomolecular solvation and electrostatics make a trade-off between these opposing considerations of atomic accuracy and computational expense.

A variety of computational methods have been developed for studying electrostatic interactions in biomolecular systems. Popular methods for understanding electrostatic interactions in these systems can be loosely classified into two categories (see Fig. 1): explicit solvent methods (Burkert and Allinger, 1982; Horn *et al.*, 2004; Jorgensen *et al.*, 1983; Ponder and Case, 2003; Sagui and Darden, 1999), which treat the solvent in full atomic detail, and implicit solvent methods (Baker, 2005b; Baker *et al.*, 2006; Davis and McCammon, 1990b; Honig and Nicholls, 1995; Roux, 2001; Roux and Simonson, 1999), which represent the solvent through its average effect on solute.

A. Explicit Solvent Methods

Explicit solvent methods offer a very detailed description of biomolecular solvation. In explicit solvent methods, interactions between mobile ions, solvent, and solute atoms are typically described by molecular mechanics force fields (Ponder and Case, 2003; Wang *et al.*, 2001b), which use classical approximations of quantum mechanical energies to describe the Coulombic (electrostatic), van der Waals, and covalent (bond, angle) interactions. Explicit solvent methods have the obvious advantage of offering the full details of solvent–solute and solvent–solvent interactions. These details can affect some aspects of biomolecular interactions.

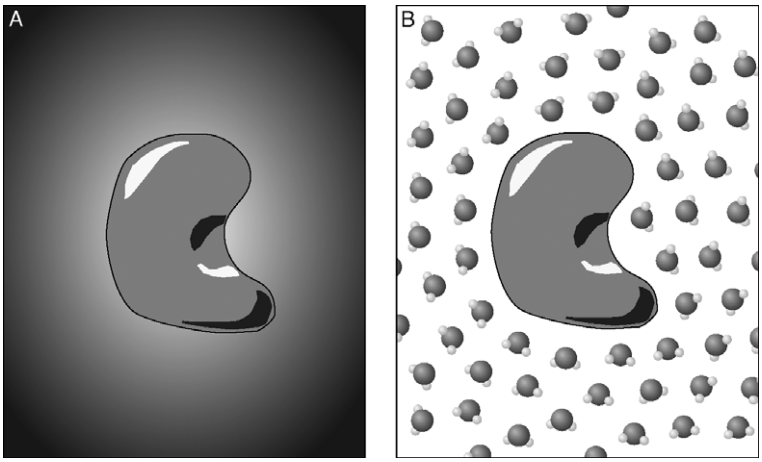

Fig. 1 A schematic comparison of implicit and explicit solvent models. (A) In the implicit solvent model, a low dielectric solute is surrounded by a continuum of high dielectric solvent. (B) In the explicit solvent model, solvent is represented by discrete water molecules.

For example, the explicit representation of solvent structure can qualitatively change the detailed features of protein side chain interactions (Masunov and Lazaridis, 2003). Similarly, Yu *et al*. have demonstrated the importance of including first shells of solvation to correctly describe the interaction of salt bridges in solution (Yu *et al*., 2004).

However, the explicit solvent methods are computationally expensive. In order to extract meaningful thermodynamic and kinetic parameters, all the numerous conformations of biomolecules, as well as the solvent and ions, must be explored. The extra degrees of freedom associated with the explicit solvent and ions dramatically increase the computational cost of explicit solvent methods and limit the temporal and spatial scales of biomolecular simulations.

B. Implicit Solvent Methods

Implicit solvent methods have become popular alternatives to the computationally expensive explicit solvent approaches although they have a lower accuracy (Baker, 2005b; Baker *et al*., 2006; Davis and McCammon, 1990b; Gilson, 2000; Honig and Nicholls, 1995; Roux, 2001). In implicit solvent methods, the molecules of interest are treated explicitly while the solvent is represented by its average effect on the solute (Roux and Simonson, 1999). Solute–solvent interactions are described by solvation energies; that is, the free energy of transferring the solute from a vacuum to the solvent environment of interest (e.g., water at a certain ionic strength). This process is shown in more detail in Fig. 2. The process consists of three steps: (1) solute charges are gradually reduced to zero in vacuum, (2) the uncharged solute is inserted into the solvent, and (3) solute charges are gradually

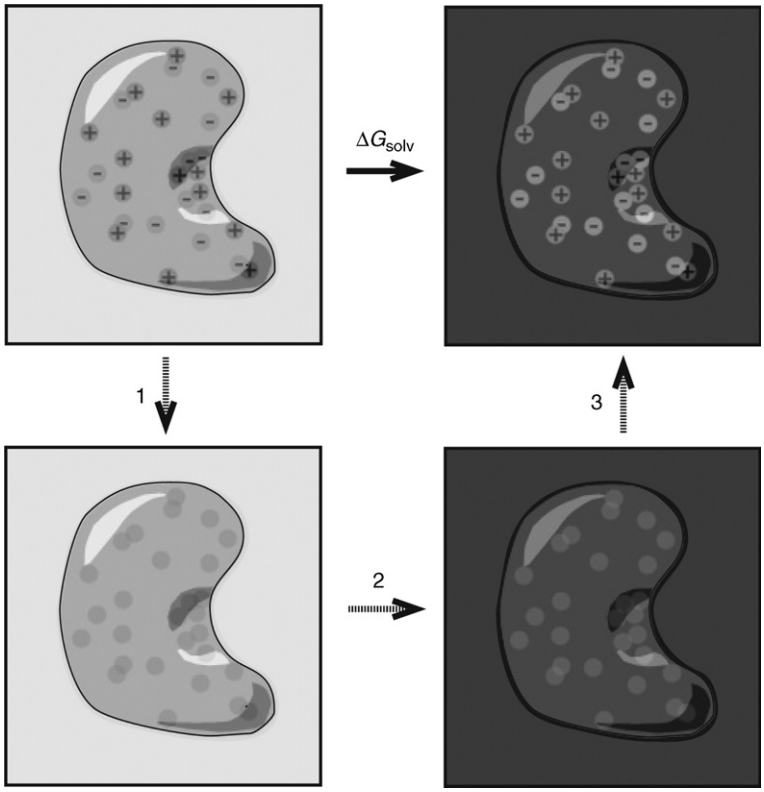

Fig. 2 A thermodynamic cycle illustrating the biomolecular solvation process. The steps are (1) uncharging the biomolecule in vacuum, (2) transferring the uncharged biomolecule from vacuum to solvent, and (3) charging the biomolecule back to its normal value in solvent. The nonpolar solvation free energy is the free energy change in step (2). The polar solvation free energy is the sum of the free energy changes in steps (1) and (3).

increased back to their normal values in the solvent. The free energy change in step (2) is called the nonpolar solvation energy. The sum of the energies associated with steps (1) and (3) is called the "charging" or polar solvation energy and represents the solvent's effect on the solute charging process. In general, polar and nonpolar solvation terms act in opposing directions; nonpolar solvation favors compact structures with small areas and volumes, while polar solvation favors maximum solvent exposure for all polar groups in the solute.

1. Nonpolar Solvation

One popular approximation for the nonpolar solvation free energy assumes a linear dependence between the nonpolar solvation energy, $G_{solv}^{nonpolar}$, and the solvent-accessible surface area (SASA), A (Chothia, 1974; Eisenberg, 1976;

Massova and Kollman, 2000; Sharp *et al.*, 1991; Spolar *et al.*, 1989; Swanson *et al.*, 2004; Wesson and Eisenberg, 1992):

$$G_{\text{solv}}^{\text{nonpolar}} = \gamma \cdot A \tag{1}$$

where γ is a "surface tension" which is typically chosen to reproduce the nonpolar solvation free energy of alkanes (Sharp *et al.*, 1991; Simonson and Brunger, 1994; Sitkoff *et al.*, 1994b) or model side chain analogues (Eisenberg and McLachlan, 1986; Wesson and Eisenberg, 1992). The surface tension parameter may assume a single global value used for all atom types or different values may be assigned to each different type of atom. Although SASA methods have enjoyed surprising success, they are also subject to several caveats, including widely varying choices of surface tension parameter (Chothia, 1974; Eisenberg and McLachlan, 1986; Elcock *et al.*, 2001; Sharp *et al.*, 1991; Sitkoff *et al.*, 1994a) as well as inaccurate descriptions of the detailed aspects of nonpolar solvation energy (Gallicchio and Levy, 2004), peptide conformations (Su and Gallicchio, 2004), and protein nonpolar solvation forces (Wagoner and Baker, 2004). Some of these problems have been fixed by new models which include the small but important attractive van der Waals interactions between solvent and solute (Gallicchio and Levy, 2004; Gallicchio *et al.*, 2000, 2002; Wagoner and Baker, 2006) as well as repulsive solvent-accessible volume terms (Wagoner and Baker, 2006).

2. Polar Solvation

Implicit solvent methods have been used to study polar solvation and electrostatics for over 80 years, starting with work by Born on ion solvation (1920), Linderström-Lang (1924) and Tanford and Kirkwood (1957) on protein titration, Manning on ion distributions surrounding nucleic acids (1978), Flanagan *et al.* (1981) on the pH dependence of hemoglobin dimer assembly, and Warwicker and Watson (1982) on the electrostatic potential of realistic protein geometries. Although they can be considerably different in their details and implementation, implicit solvent models generally treat the solvent as a high dielectric continuum, the aqueous ions as a diffuse cloud of charge, and the solute as a fixed array of point charges that are embedded in a lower dielectric continuum. Despite the limitations of these assumptions, implicit solvent models often give a good coarse-grained description of solvation energetics and have enjoyed widespread use over recent years.

Regardless of the particular type of implicit solvent model, the behavior of electrostatic interactions is generally determined by a few basic properties of the system, illustrated in Fig. 3: the charges, radii, and "dielectric constant" of the solute; the charges and radii of aqueous ionic species; and the radii and dielectric constant of the solvent. The relationship of these specific parameters to solvation energies and forces will be described in more detail in Sections III.C and III.D.

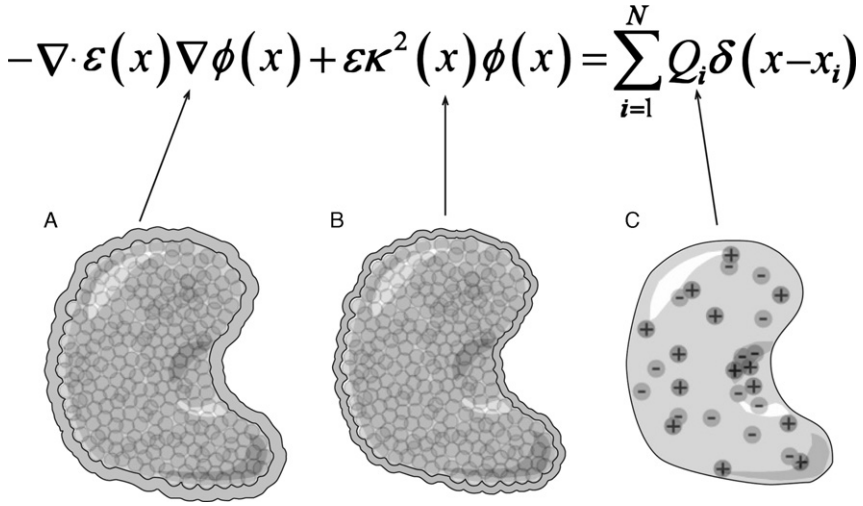

Fig. 3 Description of the terms in the Poisson–Boltzmann equation: (A) the dielectric permittivity coefficient $\varepsilon(\vec{x})$ is much smaller inside the biomolecule than outside the biomolecule, with a rapid change in value across the solvent-accessible biomolecular surface, (B) the ion-accessibility parameter $\kappa^2(\vec{x})$ is proportional to the bulk ionic strength outside the ion-accessible biomolecular surface, and (C) the biomolecular charge distribution is defined as the collection of point charges located at the center of each atom.

C. Poisson–Boltzmann Methods

The Poisson–Boltzmann (PB) equation is a popular continuum description of electrostatics for the biomolecular system. Although there are a number of ways to derive the PB equation based on statistical mechanics (Holm *et al.*, 2001), the simplest derivation begins with Poisson's equation (Bockris and Reddy, 1998; Jackson, 1975) (in SI units),

$$-\nabla\cdot\varepsilon(\vec{x})\nabla\phi(\vec{x}) = \rho(\vec{x}) \tag{2}$$

the basic equation for describing the electrostatic potential $\phi(\vec{x})$ at point $\vec{x}$ generated by a charge distribution $\rho(\vec{x})$ in an environment with a dielectric permittivity coefficient $\varepsilon(\vec{x})$ (Jackson, 1975; Landau *et al.*, 1982).

The coefficient $\varepsilon(\vec{x})$ is given by $\vec{x}$ where $\varepsilon_0 = 8.8542 \times 10^{-12}$ C^2/Nm^2 is the electrostatic permittivity of vacuum and $\varepsilon_r(\vec{x})$ is the dielectric coefficient or the relative electrostatic permittivity. The dielectric coefficient $\varepsilon_r(\vec{x})$ describes the local polarizability of the material: that is, the generation of local dipole densities in response to the applied fields and changes in charge. The functional form of this coefficient depends on the shape of the biomolecule; $\varepsilon_r(\vec{x})$ assumes lower values of 2–20 in the biomolecular interior and higher values of ~80, the value for

water at room temperature, in solvent-accessible regions. The distinction between biomolecular "interior" and "exterior" used to assign dielectric coefficients is imprecise; as a result, a variety of different definitions for the biomolecular surface and dielectric coefficient have been developed (Connolly, 1985; Grant *et al.*, 2001; Im *et al.*, 1998; Lee and Richards, 1971; Warwicker and Watson, 1982).

In order to continue the derivation of the PB equation, we assume the charge distribution $\rho(\vec{x})$ includes two contributions: the solute charges $\rho_{\mathrm{f}}(\vec{x})$ and the aqueous "mobile" ions $\rho_{\mathrm{m}}(\vec{x})$. The solute charge distribution is generally described by a collection of N point charges located at each solute atom's position $\vec{x}_i$ and scaled by that atom's charge Q_i; that is, the solute charge distribution is the summation of a set of delta functions $\rho_f(\vec{x}) = \sum_i Q_i \delta(\vec{x} - \vec{x}_i)$. Neglecting explicit interactions between the aqueous ions (Holm *et al.*, 2001), the mobile charges are modeled as a continuous "charge cloud" described by a Boltzmann distribution (McQuarrie, 2000). For m ion species with charges q_j, bulk concentrations c_j, and steric potential $V_j(\vec{x})$ (a potential that prevents biomolecule–ion overlap), the mobile ion charge distribution is $\rho_{\mathrm{m}}(\vec{x}) = \sum_j^m c_j q_{\mathrm{j}} \exp[-q_j\phi(\vec{x})/k_{\mathrm{B}}T - V_j(\vec{x})/k_{\mathrm{B}}T]$, where k_{B} is Boltzmann's constant and T is the absolute temperature. Combining both the solute and ion charge distributions with the Poisson equation, Eq. (2), gives the full PB equation:

$$-\nabla\cdot\varepsilon(\vec{x})\nabla\phi(\vec{x}) = \sum_{i=1}^{N} Q_i\delta(\vec{x}-\vec{x}_i) + \sum_{j=1}^{m} c_j q_{\mathrm{j}} \exp[-q_j\phi(\vec{x})/k_{\mathrm{B}}T - V_j(\vec{x})/k_{\mathrm{B}}T] \quad (3)$$

A common simplification is that the exponential term $\exp[-q_j\phi(\vec{x})/k_{\mathrm{B}}T]$ can be approximated by the linear term in its Taylor series expansion $-q_j\phi(\vec{x})/k_{\mathrm{B}}T$ for $|q_j\phi(\vec{x})/k_{\mathrm{B}}T| \ll 1$. With this linearization and by assuming the steric occlusions are the same for all ion species ($V_j = V$ for all j), Eq. (3) reduces to the linearized PB equation:

$$-\nabla\cdot\varepsilon(\vec{x})\nabla\phi(\vec{x}) + \varepsilon(\vec{x})\kappa^2(\vec{x})\phi(\vec{x}) = \sum_{i=1}^{N} Q_i\delta(\vec{x}-\vec{x}_i) \quad (4)$$

where $\kappa^2(\vec{x})$, related to a modified inverse Debye–Hückel screening length (Debye and Hückel, 1923), is given by

$$\kappa^2(\vec{x}) = \exp\left[\frac{-V(\vec{x})}{k_{\mathrm{B}}T}\right]\cdot\frac{2Ie_c^2}{k_{\mathrm{B}}T\varepsilon(\vec{x})} \quad (5)$$

where $I = 1/2\sum_j^m c_j q_j^2/e_{\mathrm{c}}^2$ is the ionic strength and e_{c} is the unit electric charge.

Once the PB equation is solved, the electrostatic potential is known for the entire system. Given this potential, the electrostatic free energy can be evaluated by a

variety of integral formulations (Gilson, 1995; Micu *et al.*, 1997; Sharp and Honig, 1990). The simplest, for the linearized PB equation, is

$$G_{\text{el}} = \frac{1}{2}\sum_{i=1}^{N} Q_i \phi(\vec{x}_i) \tag{6}$$

It is also possible to differentiate integral formulations of the electrostatic energy with respect to atomic position to obtain the electrostatic or polar solvation force on each atom (Gilson *et al.*, 1993; Im *et al.*, 1998).

Analytical solutions of the PB equation are not available for biomolecules with realistic shapes and charge distributions. Numerical methods for solving the PB equation were first introduced by Warwicker and Watson (1982) to obtain the electrostatic potential at the active site of an enzyme. The most common numerical techniques for solving the PB equation are based on discretization of the domain of interest into small regions. Those methods include finite difference (Baker *et al.*, 2001; Davis and McCammon, 1989; Holst and Saied, 1993, 1995; Nicholls and Honig, 1991), finite element (Baker *et al.*, 2000, 2001; Cortis and Friesner, 1997a,b; Dyshlovenko, 2002; Holst *et al.*, 2000), and boundary element methods (Allison and Huber, 1995; Bordner and Huber, 2003; Boschitsch and Fenley, 2004; Juffer *et al.*, 1991; Zauhar and Morgan, 1988), all of which continue to be developed to further improve the accuracy and efficiency of electrostatics calculations in the numerous biomolecular applications described below. The major software packages that can be used to solve the PB equation are listed in Table I. Many of these packages are also used for visualization of the electrostatic potential around biomolecules. Such visualization can provide insight into biomolecular function and highlight regions of potential interest. Figure 4 shows examples of the visualization of electrostatic potential calculated with Adaptive Poisson-Boltzmann solver (APBS) (Baker *et al.*, 2001) and visualized with Visual Molecular Dynamics (VMD) (Humphrey *et al.*, 1996).

Table I
Major PB Equation Solver

Software package	URL
APBS (Baker *et al.*, 2001)	http://apbs.sf.net/
Delphi (Rocchia *et al.*, 2001)	http://trantor.bioc.columbia.edu/delphi/
MEAD (Bashford, 1997)	http://www.scripps.edu/mb/bashford/
ZAP (Grant *et al.*, 2001)	http://www.eyesopen.com/products/toolkits/zap.html
UHBD (Madura *et al.*, 1995)	http://mccammon.ucsd.edu/uhbd.html
Jaguar (Cortis and Friesner, 1997a,b)	http://www.schrodinger.com/
CHARMM (MacKerell *et al.*, 1998)	http://yuri.harvard.edu
Amber (Luo *et al.*, 2002)	http://amber.scripps.edu

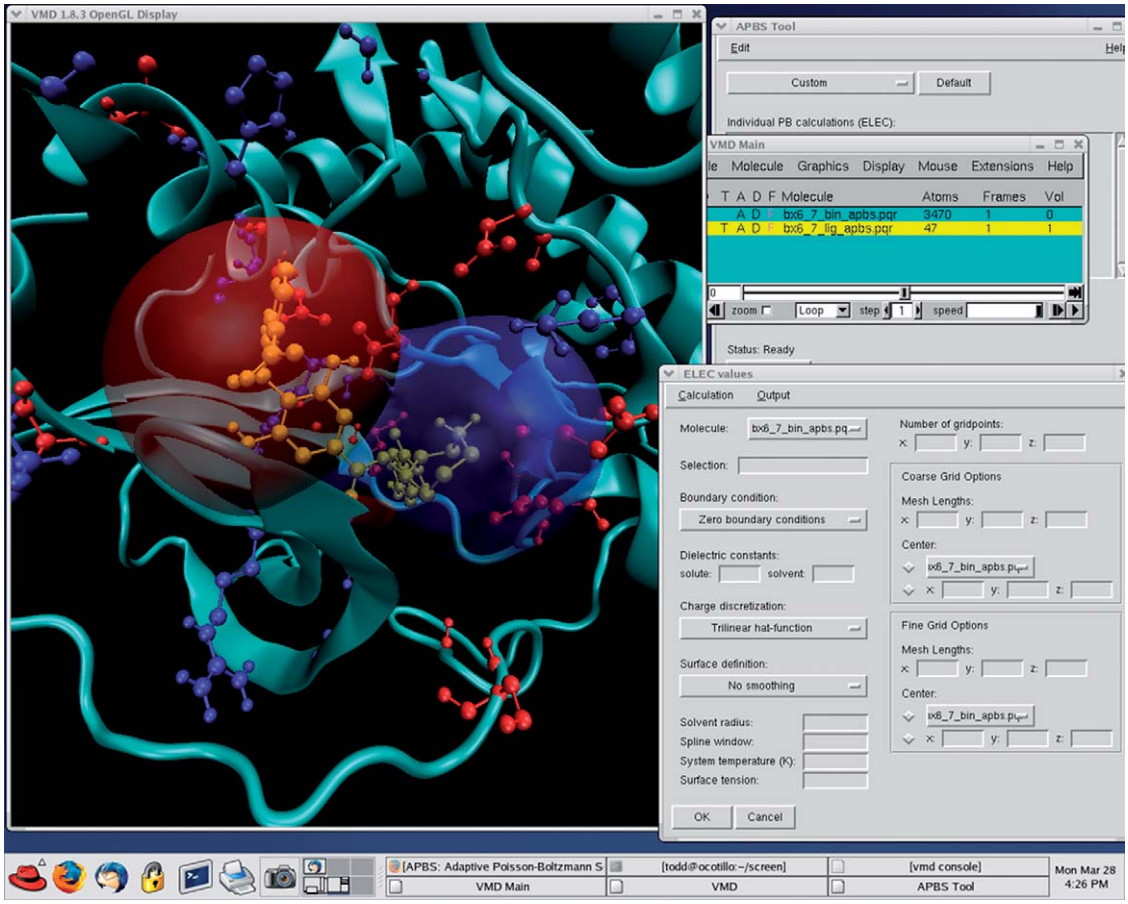

Fig. 4 Examples of the visualization of the balanol electrostatic potential in the binding site of protein kinase A as calculated by APBS (Baker *et al.*, 2001) and visualized with VMD (Humphrey *et al.*, 1996).

D. Simpler Models

In addition to the PB methods, simpler approximate models have also been constructed for continuum electrostatics, including distance-dependent dielectric functions (Leach, 2001; MacKerell and Nilsson, 2001), analytic continuum methods (Schaeler and Karplus, 1996), and generalized Born (GB) models (Bashford and Case, 2000; Dominy and Brooks, 1999; Onufriev *et al.*, 2002; Osapay *et al.*, 1996; Still *et al.*, 1990). Among these simpler methods, GB is currently the most popular. The GB model was introduced by Still *et al.* in 1990 and subsequently refined by several other researchers (Bashford and Case, 2000; Dominy and Brooks, 1999; Onufriev *et al.*, 2002; Osapay *et al.*, 1996). The model shares the same continuum representation of the solvent as the Poisson or PB theories.

However, the GB model is based on the analytical solvation energy obtained from the solution of the Poisson equation for a simple sphere (Born, 1920). The biomolecular electrostatic solvation free energy is approximated by a modified form of the analytical solvation energy for a sphere (Still *et al.*, 1990):

$$\Delta G_{\text{solv}}^{\text{el}} \cong -\frac{1}{2}\left(1-\frac{1}{\varepsilon_{\text{sol}}}\right)\sum_{i,j}\frac{Q_iQ_j}{f_{ij}^{\text{GB}}} \tag{7}$$

where the self terms as $i=j$, f_{ij}^{GB}, are the "effective Born radii" and the cross terms as $i\neq j$, f_{ij}^{GB}, are the effective interaction distances. The most common form of f_{ij}^{GB} (Still *et al.*, 1990) is

$$f_{ij}^{\text{GB}} = \left[r_{ij}^2 + R_iR_j\,\exp\left(\frac{-r_{ij}^2}{4R_iR_j}\right)\right]^{1/2} \tag{8}$$

where R_i are the effective radii of the atoms and r_{ij} are the distance between atoms i and j. Efficiently and accurately calculating the effective radii is essential for GB methods. "Perfect" GB radii, which reproduce atom i's self-energy obtained by solving the Poisson equation for the biomolecule–solvent system with only atom i charged, have demonstrated the ability to accurately follow the results of more detailed models such as PB (Onufriev *et al.*, 2002). However using such "perfect" radii does not directly provide any computational advantage over solving the Poisson equation. In the absence of perfect radii for every biomolecular conformation, GB methods fail to capture some aspects of molecular structure included in more detailed models, such as the PB equation. Nonetheless, GB methods have become increasingly popular because of their computational efficiency.

E. Limitations of Implicit Solvent Methods

Although implicit solvent methods offer simpler descriptions of the system and greater computational efficiency, it is important to recall that these reductions of complexity and effort are obtained at the cost of substantial simplification of the description of the solvent. In particular, implicit solvent methods are capable of describing only nonspecific interactions between solvent and solute. In general, explicit solvent methods should be used wherever the detailed interactions between solvent and solute are important, such as solvent finite size effects in ion channels (Nonner *et al.*, 2001), strong solvent–solute interactions (Bhattacharrya *et al.*, 2003), strong solvent coordination of ionic species (Figueirido *et al.*, 1994; Yu *et al.*, 2004), and saturation of solvent polarization near a membrane (Lin *et al.*, 2002). Similarly, as mentioned earlier in the context of RNA–ion interactions, implicit descriptions of mobile ions can also become questionable in some cases, such as high ion valency or strong solvent coordination, specific ion–solute

interactions, and high local ion densities (Holm *et al.*, 2001), where the ions interact with each other or with the solute directly.

IV. Applications

In the previous section, we discussed the basic concepts behind the computational tools that can be used to simulate electrostatic interactions in cellular systems. In this section, we will illustrate the use of these methods, especially PB methods, to deal with the various biomolecular problems.

A. Solvation Free Energy

As mentioned in Section III.B, the solvation free energy is the free energy of transferring a solute from a uniform dielectric continuum (a constant dielectric) to an inhomogeneous medium (a low dielectric solute surrounded by a high dielectric solvent), which is often divided into two terms: a nonpolar term and a polar term. The nonpolar term is usually estimated using either SASA or the improved methods discussed in Section III.B.1. For the polar term, as shown in Fig. 5, two PB calculations are usually performed: (1) calculating the biomolecular electrostatic free energy, $G_{el}^{(1)}$, in a homogeneous medium with a constant dielectric equal to the solute's dielectric coefficient and (2) calculating the biomolecular electrostatic free energy, $G_{el}^{(2)}$, in the inhomogeneous medium of interest, for example, a protein in aqueous medium. The polar contribution to the solvation free energy is then given by

$$\Delta G_{solv}^{polar} = G_{el}^{(2)} - G_{el}^{(1)} \tag{9}$$

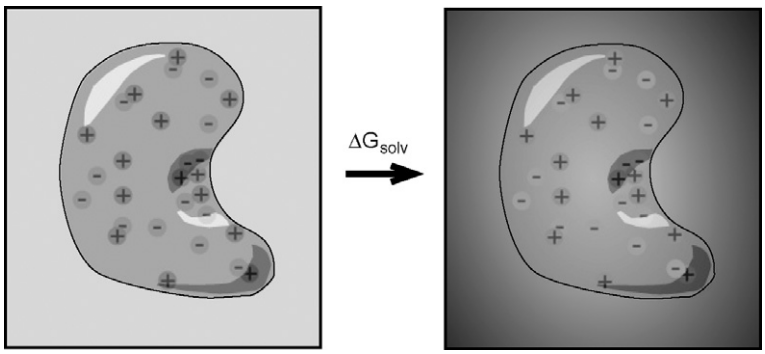

Fig. 5 Schematic of a polar solvation free energy calculation; in the initial state, the dielectric coefficient is a constant throughout the entire system and equal to the solute's dielectric coefficient; in the final state, the dielectric coefficient is inhomogeneous and smaller in the solute than in the bulk solvent.

Additionally, solving the PB equation twice helps to cancel the numerical artifacts which arise from the discretization used in finite difference and finite element methods; that is, it reduces the grid size dependence. Although, in most cases, polar solvation free energy alone is not sufficient to explain the biological phenomenon, it is the foundation for the other, more complex, electrostatic calculations described below.

B. Electrostatic Free Energy

The total electrostatic free energy can be easily obtained from the polar solvation free energy by adding the electrostatic free energy of the biomolecule in a homogeneous medium with a constant dielectric equal to the solute's dielectric coefficient using Coulomb's law:

$$G_{\text{el}} = \Delta G_{\text{solv}}^{\text{polar}} + G_{\text{coul}} \tag{10}$$

where

$$G_{\text{coul}} = \sum_{i,j} \frac{1}{4\pi\varepsilon_0\varepsilon_p} \cdot \frac{Q_i Q_j}{r_{ij}} \tag{11}$$

where r_{ij} is the distance between charge Q_i and Q_j and ε_p is the dielectric coefficient of the solute. The resulting electrostatic free energies are the basis for nearly all applications of continuum electrostatics methods to biomolecular systems.

As a specific example, such electrostatic free energy calculations have been used to study the electrostatic sequestration of phosphatidylinositol 4,5-bisphosphate (PIP_2) by membrane-adsorbed basic peptides (Wang *et al.*, 2004). PIP_2 is a very important lipid in the cytoplasmic leaflet of the plasma membrane (Cantley, 2002; De Camilli *et al.*, 1996; Irvine, 2002; Martin, 2001; McLaughlin *et al.*, 2002; Payrastre *et al.*, 2001; Raucher *et al.*, 2000; Toker, 1998; Yin and Janmey, 2003) with a net charge of –4e on the lipid head group. By calculating the electrostatic free energy of laterally sequestering a PIP_2 lipid from a region of "bulk" membrane to a region in the vicinity of a membrane-absorbed basic peptide, Wang *et al* demonstrated that nonspecific electrostatic interactions provide a driving force for the lateral sequestration of PIP_2 by membrane-adsorbed basic peptides (Rauch *et al.*, 2002; Wang *et al.*, 2001a, 2002, 2004). Such lateral sequestration of PIP_2 is thought to contribute to the regulation of PIP_2 function by controlling its accessibility to other proteins (Laux *et al.*, 2000; McLaughlin *et al.*, 2002).

C. Folding Free Energies

Biomolecular native (folded) structure is very important for proper performance of their biological functions. However, accurately determining the mechanism by which electrostatic interactions affect the stability of bimolecular native structure is

still a challenging experimental and computational question. The electrostatic contribution to the biomolecular folding stability is usually defined as the difference in electrostatic free energy between folded (G^{el}_{folded}) and unfolded ($G^{el}_{unfolded}$) states:

$$\Delta G^{el}_{folding} = G^{el}_{folded} - G^{el}_{unfolded} \tag{12}$$

If $\Delta G^{el}_{folding} < 0$, from the electrostatic point of view, the folded structure is more stable than the unfolded structure. If $\Delta G^{el}_{folding}$ reduces in response to a mutation, that is, if $\Delta\Delta G^{el}_{folding} = \Delta G^{el,m}_{folding} - \Delta G^{el,w}_{folding} < 0$, this mutation makes the folded protein more stable. This method has been widely used to study electrostatic contribution to protein folding stabilities through mutations that involve charged or polar residues. For example, *Bacillus caldolyticus* cold shock protein (Bc-Csp) is a thermophilic protein that differs from *B. subtilis* cold shock protein B (Bs-CspB), its mesophilic homologue, in 11 of its 66 residues (Delbruck *et al.*, 2001; Mueller *et al.*, 2000). Through mutational studies, which reduced the sequence differences between these two protein molecules, both experimental (Delbruck *et al.*, 2001; Mueller *et al.*, 2000; Pace, 2000; Perl *et al.*, 2000; Perl and Schmid, 2001) and PB calculations (Zhou and Dong, 2003) demonstrated that the difference in stability of these two proteins arises mostly from the interactions among the three residues: Arg 3, Glu 46, and Leu 66 in Bc-Csp, as compared with Glu 3, Ala 46, and Glu 66 in Bs-CspB. The removal of the repulsion between Glu 3 and Glu 66 and the creation of a favorable salt bridge between Arg 3 and Glu 46 are the main reasons that Bc-Csp is more stable than Bs-CspB at higher temperatures. Moreover, the excellent agreement between PB calculations and experimental data (the correlation coefficient is 0.98) implies that electrostatic interactions dominate the thermostability of thermophilic proteins (Zhou and Dong, 2003).

D. Binding Free Energies

The binding of biomolecules is fundamental to cellular activity. The simplest type of binding energy calculations are performed on the biomolecular complex assuming a rigid conformation; that is, without any conformational changes on binding, which is clearly not realistic, but often provides useful initial estimates for relative biomolecular binding affinities. Figure 6 illustrates the procedure to calculate the polar contribution to the binding free energy, $\Delta G^{el}_{binding}$, which is given by

$$\begin{aligned}\Delta G^{el}_{binding} &= G^{el}_{complex} - (G^{el}_{mol1} + G^{el}_{mol2}) \\ &= [\Delta G^{solv}_{complex} - (\Delta G^{solv}_{mol1} + \Delta G^{solv}_{mol2})] + [G^{coul}_{complex} - (G^{coul}_{mol1} + G^{coul}_{mol2})] \\ &= \Delta\Delta G^{solv}_{binding} + \Delta G^{coul}_{binding}\end{aligned} \tag{13}$$

where $\Delta\Delta G^{solv}_{binding} = \Delta G^{solv}_{complex} - (\Delta G^{solv}_{mol1} + \Delta G^{solv}_{mol2})$ is the polar solvation free energy change on binding with the ΔG^{solv}_{i} values calculated according to Eq. (9) above.

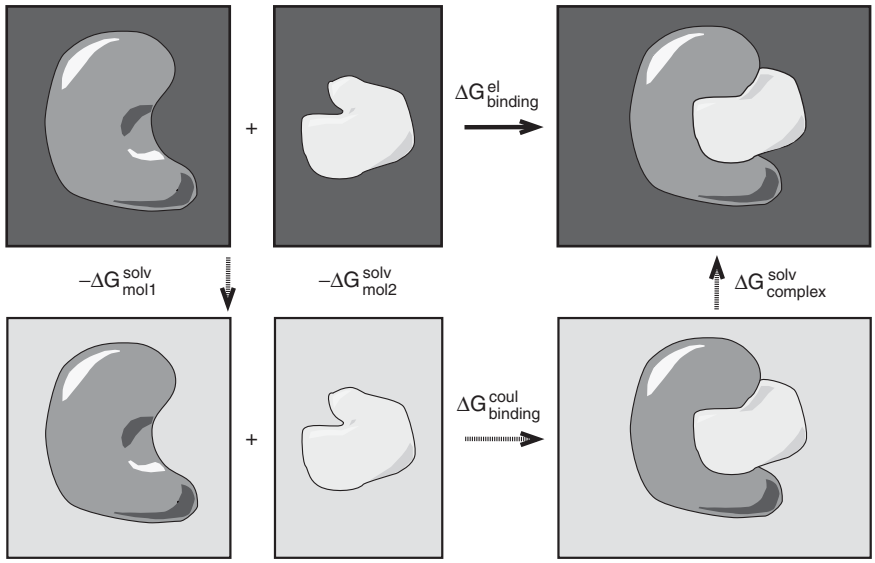

Fig. 6 Thermodynamic cycle illustrating the standard procedure for calculating the electrostatic contribution to the binding free energy of a complex with rigid body. The steps are as follows: (1) transfer the isolated molecule from a inhomogeneous dielectric into a homogeneous dielectric, the free energy change is $-(\Delta G^{\text{solv}}_{\text{mol1}} + \Delta G^{\text{solv}}_{\text{mol2}})$; (2) form the complex from isolated molecules in a homogeneous dielectric, the free energy change is $\Delta G^{\text{coul}}_{\text{binding}}$, (3) transfer the complex from the homogeneous dielectric into the inhomogeneous dielectric, the free energy change is $\Delta G^{\text{solv}}_{\text{complex}}$.

The quantity $\Delta G^{\text{coul}}_{\text{binding}} = G^{\text{coul}}_{\text{complex}} - (G^{\text{coul}}_{\text{mol1}} + G^{\text{coul}}_{\text{mol2}})$ is the Coulombic free energy change on binding with the $\Delta G^{\text{coul}}_{i}$ values calculated according to Eq. (11) above.

For the more general situation in which biomolecules experience conformational changes during the binding process, MM/PBSA and MM/GBSA methods (Kollman *et al.*, 2000; Swanson *et al.*, 2004) are commonly used to calculate the binding free energy. The nature of these methods can be best understood through their acronym: MM stands for the molecular mechanics force fields used to calculate the intramolecular and direct intermolecular contributions to binding free energies; PB and GB refer to the implicit solvent methods used to calculate the electrostatic contributions, and SA stands for SASA methods used to calculate the nonpolar contributions to binding free energies.

Binding free energy calculations using continuum solvation models have been successfully performed on many different biomolecular complexes (Dong *et al.*, 2003; Eisenberg and McLachlan, 1986; Green and Tidor, 2005; Massova and Kollman, 2000; Misra *et al.*, 1998; Murray *et al.*, 1997; Sept *et al.*, 1999, 2003; Wang *et al.*, 2004; Wong *et al.*, 2001). As specific examples, binding free energy calculations have been performed to investigate the roles of charged residues at the interface of barnase (an extracellular ribonuclease) and barstar (a protein inhibitor), which have been a popular test case for both computational

(Dong *et al.*, 2003; Gabdoulline and Wade, 1997, 1998, 2001; Lee and Tidor, 2001; Sheinerman and Honig, 2002; Spaar and Helms, 2005; Spaar *et al.*, 2006; Wang and Wade, 2003) and experimental studies of protein–protein interactions (Frisch *et al.*, 1997; Schreiber and Fersht, 1993, 1995). In particular, PB calculations (Dong *et al.*, 2003) successfully reproduced the experimental result (Frisch *et al.*, 1997; Schreiber and Fersht, 1993, 1995) that cross-interface salt bridges and hydrogen bonds dominate the binding affinities of barnase and barstar (Dong *et al.*, 2003).

E. pK_a Calculations

The presence of ionizable sites, which can exchange protons with their environment, produces pH-dependent phenomena in proteins and has a significant influence on the protein's function. The correct prediction of protein titration states is important for the analysis of enzyme mechanisms, protein stability, and molecular recognition. As mentioned earlier, efforts have been underway for more than 80 years (Alexov, 2003; Antosiewicz *et al.*, 1996b; Bastyns *et al.*, 1996; Fitch *et al.*, 2002; Georgescu *et al.*, 2002; Jensen *et al.*, 2005; Krieger *et al.*, 2006; Li *et al.*, 2002, 2004; Linderström-Lang, 1924; Luo *et al.*, 1998; Nielsen and McCammon, 2003; Nielsen and Vriend, 2001) to correctly predict protein titration states and understand the determinants of pK_as for amino acids in protein environments (see chapter 26 by Whitten *et al.*, this volume).

The free energy change, ΔG, for protonation of a single ionizable site at a given pH may be written as (Linderström-Lang, 1924; Tanford and Kirkwood, 1957)

$$\Delta G = G^{\text{el}}_{\text{protonated}} - G^{\text{el}}_{\text{deprotonated}} = (k_B T \ln 10)(\text{pH} - \text{p}K_a) \tag{14}$$

where $\text{p}K_a = -\log_{10} K_a$ and $K_a = [H^+][A^-]/[HA]$ is the equilibrium constant for the dissociation of proton H^+ and its conjugate site A^-; k_B is Boltzmann's constant; and T is the absolute temperature. A widely used assumption in pK_a predictions is that any pK_a differences of an ionizable site when located in a protein versus in a model compound are solely determined by the difference in the electrostatic free energy required to protonate that site in the protein versus the model compound. Thus, the p$K_a$of the single ionizable site in protein is given by

$$\text{p}K_a = \text{p}K_0 - \Delta\Delta G/(k_B T \ln 10) \tag{15}$$

where $\Delta\Delta G = \Delta G_{\text{protein}} - \Delta G_{\text{model}}$ and pK_0 is the pK_a of the isolated ionizable site in the model compound. In general, proteins have multiple ionizable sites and the protonation energetics of these different sites are coupled, as discussed below. Single-site pK_a predictions have successfully reproduced measured pK_as for different residues in several different proteins (Dong and Zhou, 2002; Dong *et al.*, 2003)

and therefore have some predictive power. However, a more complete treatment of ionizable residues in proteins considers the coupling between all the ionizable sites. There are a number of techniques for treating such coupling (Antosiewicz *et al.*, 1996a,b; Bashford, 2004; Beroza *et al.*, 1991; Tanford and Roxby, 1972), and thereby determining the complete titration state of the protein. Unfortunately, such methods are complex and are beyond the scope of the current discussion.

F. Biomolecular Association Rates

BD calculations are popular methods to simulate the relative diffusional motion between two solute particles and thereby estimate the rate of diffusion-controlled binding between two molecules (Ermak and McCammon, 1978; Northrup *et al.*, 1984). Given the importance of electrostatic interactions in biomolecular association, BD simulations are usually combined with continuum electrostatic calculations to provide the most accurate estimates of diffusion-limited encounter rates (Allison and McCammon, 1985; Davis and McCammon, 1990a; Gabdoulline and Wade, 2001, 2002; Ilin *et al.*, 1995; Madura *et al.*, 1995; Sept *et al.*, 1999). Such calculations have been used in numerous diffusional encounter rate calculations, including simulations of small molecule interactions with enzymes (Allison and McCammon, 1985; Davis *et al.*, 1991; Elcock *et al.*, 1996; Luty *et al.*, 1993; Madura and McCammon, 1989; Radic *et al.*, 1997; Sines *et al.*, 1992; Tan *et al.*, 1993; Tara *et al.*, 1998), simulations of protein–protein encounter (Elcock *et al.*, 1999, 2001; Gabdoulline and Wade, 1997, 2001; Sept *et al.*, 1999; Spaar *et al.*, 2006), as well as functional assessment of differences in protein electrostatics (Livesay *et al.*, 2003).

V. Conclusion and Future Directions

Computer simulation is becoming an increasingly routine way to help with drug discovery or other applications requiring a detailed understanding of molecular interactions. A correct understanding of the energetic interactions within and between biomolecules is essential for such simulations. Among the various contributions to these energies, electrostatic interactions are of special importance because of their long range and strength. In this chapter, we have covered some of the computational methods that are currently available to model the electrostatic interactions in biomolecular systems, ranging from highly detailed explicit solvent methods to simpler PB and GB methods. There are several reviews available on all of these methods which provide a more in-depth discussion of the different solvation approaches. The reviews of Ponder and Case (2003) as well as the texts of Becker *et al.* (2001), Leach (2001), and Schlick (2002) provide excellent background on explicit solvent methods. There also are several reviews available for implicit solvent methods (see Baker, 2005a; Bashford and Case, 2000; Honig and Nicholls, 1995; Roux and Simonson, 1999; Simonson, 2003), including a particularly thorough treatment by Lamm (2003), a discussion of current PB limitations by

Baker (2005b), and an up-to-date discussion of current challenges for GB methods by Feig and Brooks (2004). For additional background and more in-depth discussion of the principles and limitations of continuum electrostatics, interested readers should see the general volume by Jackson (1975) and Landau *et al.* (1982), the electrochemistry text of Bockris *et al.* (1998), the colloid theory treatise by Verwey and Overbeek (1999), or the excellent collection of condensed matter electrostatics articles assembled by Holm *et al.* (2001).

Acknowledgments

The authors thank Baker group members for their reading of this manuscript. This work was supported by National Institutes of Health grant R01 GM069702.

References

Alexov, E. (2003). Role of the protein side-chain fluctuations on the strength of pair-wise electrostatic interactions: Comparing experimental with computed pKas. *Proteins* **50,** 94–103.

Allison, S. A., and Huber, G. A. (1995). Modeling the electrophoresis of rigid polyions: Application of lysozyme. *Biophys. J.* **68,** 2261–2270.

Allison, S. A., and McCammon, J. A. (1985). Dynamics of substrate binding to copper zinc superoxide dismutase. *J. Phys. Chem.* **89,** 1072–1074.

Anderson, C. F., and Record, M. T., Jr. (2004). Gibbs–Duhem-based relationships among derivatives expressing the concentration dependences of selected chemical potentials for a multicomponent system. *Biophys. Chem.* **112,** 165–175.

Antosiewicz, J., Briggs, J. M., Elcock, A. H., Gilson, M. K., and McCammon, J. A. (1996a). Computing ionization states of proteins with a detailed charge model. *J. Comput. Chem.* **17,** 1633–1644.

Antosiewicz, J., McCammon, A. J., and Gilson, M. K. (1996b). The determinants of pKas in proteins. *Biochemistry* **35,** 7819–7833.

Bajaj, N. P., McLean, M. J., Waring, M. J., and Smekal, E. (1990). Sequence-selective, pH-dependent binding to DNA of benzophenanthridine alkaloids. *J. Mol. Recognit.* **3,** 48–54.

Baker, N., Holst, M., and Wang, F. (2000). Adaptive multilevel finite element solution of the poisson-boltzmann equation ii. Refinement at solvent-accessible surfaces in biomolecular systems. *J. Comput. Chem.* **21,** 1343–1352.

Baker, N. A. (2005a). Biomolecular applications of Poisson-Boltzmann methods. *In* "Reviews in Computational Chemistry" (K. B. Lipkowitz, R. Larter, and T. R. Cundari, eds.), pp. 349–379. Wiley-VCH, John Wiley & Sons, Inc., Hoboken, NJ.

Baker, N. A. (2005b). Improving implicit solvent simulations: A Poisson-centric view. *Curr. Opin. Struct. Biol.* **15,** 137–143.

Baker, N. A., Bashford, D., and Case, D. (2006). Implicit solvent electrostatics in biomolecular simulation. *In* "New Algorithms for Macromolecular Simulation" (B. Leimkuhler, C. Chipot, and R. Elber, *et al.*, eds.), pp. 263–295. Springer-Verlag, Berlin.

Baker, N. A., Sept, D., Holst, M. J., and McCammon, J. A. (2001). Electrostatics of nanosystems: Application to microtubules and the ribosome. *Proc. Natl. Acad. Sci. USA* **98,** 10037–10041.

Bashford, D. (1997). Scientific computing in object-oriented parallel environments; An object-oriented programming suite for electrostatic effects in biological molecules. *In* Lecture Notes in Computer Science pp. 233–240. Springer, Berlin.

Bashford, D. (2004). Macroscopic electrostatic models for protonation states in proteins. *Front. Biosci.* **9,** 1082–1099.

Bashford, D., and Case, D. A. (2000). Generalized Born models of macromolecular solvation effects. *Annu. Rev. Phys. Chem.* **51,** 129–152.

Bastyns, K., Froeyen, M., Diaz, J. F., Volckaert, G., and Engelborghs, Y. (1996). Experimental and theoretical study of electrostatic effects on the isoelectric pH and pKa of the catalytic residue His-102 of the recombinant ribonuclease from Bacillus amyloliquefaciens (barnase). *Proteins* **24,** 370–378.

Becker, O., MacKerell, A. D., Jr., Roux, B., and Watanabe, M. (2001). ''Computational Biochemistry and Biophysics.'' Marcel Dekker, New York.

Beroza, P., Fredkin, D. R., Okamura, M. Y., and Feher, G. (1991). Protonation of interacting residues in a protein by Monte Carlo method: Application to lysozyme and the photosynthetic reaction center of Rhodobacter sphaeroides. *Proc. Natl. Acad. Sci. USA* **88,** 5804–5808.

Bhattacharrya, S. M., Wang, Z.-G, and Zewail, A. H. (2003). Dynamics of water near a protein surface. *J. Phys. Chem. B* **107,** 13218–13228.

Bockris, J. O., and Reddy, K. N. (1998). ''Modern Electrochemistry: Ionics.'' Plenum Press, New York.

Bordner, A. J., and Huber, G. A. (2003). Boundary element solution of linear Poisson-Boltzmann equation and a multipole method for the rapid calculation of forces on macromolecules in solution. *J. Comput. Chem.* **24,** 353–367.

Born, M. (1920). Volumen und hydratationswarme der ionen. *Z. Phys.* **1,** 45–48.

Boschitsch, A. H., and Fenley, M. O. (2004). Hybrid boundary element and finite difference method for solving the nonlinear Poisson-Boltzmann equation. *J. Comput. Chem.* **25,** 935–955.

Boström, M., Deniz, V., and Ninham, B. W. (2006). Ion specific surface forces between membrane surfaces. *J. Phys. Chem. B* **110,** 9645–9649.

Boström, M., Williams, D. R. M., Stewart, P. R., and Ninham, B. W. (2003). Hofmeister effects in membrane biology: The role of ionic dispersion potentials. *Phys. Rev. E* **68,** 041902–041907.

Broering, J. M., and Bommarius, A. S. (2005). Evaluation of Hofmeister effects on the kinetic stability of proteins. *J. Phys. Chem. B* **109,** 20612–20619.

Burkert, U., and Allinger, N. L. (1982). ''Molecular Mechanics.'' American Chemical Society, Washington, DC.

Cantley, L. C. (2002). The phosphoinositide 3-kinase pathway. *Science* **296,** 1655–1657.

Cech, T. R., and Bass, B. L. (1986). Biological catalysis by RNA. *Annu. Rev. Biochem.* **55,** 599–630.

Chong, L. T., Dempster, S. E., Hendsch, Z. S., Lee, L. P., and Tidor, B. (1998). Computation of electrostatic complements to proteins: A case of charge stabilized binding. *Protein Sci.* **7,** 206–210.

Chothia, C. (1974). Hydrophobic bonding and accessible surface area in proteins. *Nature* **248,** 338–339.

Cole, P. E., Yang, S. K., and Crothers, D. M. (1972). Conformational changes of transfer ribonucleic acid. Equilibrium phase diagrams. *Biochemistry* **11,** 4358–4368.

Collins, K. D. (2006). Ion hydration: Implications for cellular function, polyelectrolytes, and protein crystallization. *Biophys. Chem.* **119,** 271–281.

Connolly, M. L. (1985). Computation of molecular volume. *J. Am. Chem. Soc.* **107,** 1118–1124.

Cortis, C. M., and Friesner, R. A. (1997a). An automatic three-dimensional finite element mesh generation system for Poisson-Boltzmann equation. *J. Comput. Chem.* **18,** 1570–1590.

Cortis, C. M., and Friesner, R. A. (1997b). Numerical solution of the Poisson-Boltzmann equation using tetrahedral finite-element meshes. *J. Comput. Chem.* **18,** 1591–1608.

Dahm, S. C., and Uhlenbeck, O. C. (1991). Role of divalent metal ions in the hammerhead RNA cleavage reaction. *Biochemistry* **30,** 9464–9469.

Davis, M. E., Madura, J. D., Sines, J., Luty, B. A., Allison, S. A., and McCammon, J. A. (1991). Diffusion-controlled enzymatic reactions. *Methods Enzymol.* **202,** 473–497.

Davis, M. E., and McCammon, J. A. (1989). Solving the finite difference linearized Poisson-Boltzmann equation: A comparison of relaxation and conjugate gradient methods. *J. Comput. Chem.* **10,** 386–391.

Davis, M. E., and McCammon, J. A. (1990a). Calculating electrostatic forces from grid-calculated potentials. *J. Comput. Chem.* **11,** 401–409.

Davis, M. E., and McCammon, J. A. (1990b). Electrostatics in biomolecular structure and dynamics. *Chem. Rev.* **90,** 509–521.

De Camilli, P., Emr, S. D., McPherson, P. S., and Novick, P. (1996). Phosphoinositides as regulators in membrane traffic. *Science* **271,** 1533–1539.

Debye, P., and Hückel, E. (1923). Zur Theorie der Elektrolyte. I. Gefrierpunktserniedrigung und verwandte Erscheinungen. *Physikalische Zeitschrift* **24,** 185–206.

del Álamo, M., and Mateu, M. G. (2005). Electrostatic repulsion, compensatory mutations, and long-range non-additive effects at the dimerization interface of the HIV capsid protein. *J. Mol. Biol.* **345,** 893–906.

Delbruck, H., Mueller, U., Perl, D., Schmid, F. X., and Heinemann, U. (2001). Crystal structures of mutant forms of the *Bacillus caldolyticus* cold shock protein differing in thermal stability. *J. Mol. Biol.* **313,** 359–369.

Dominy, B. N., and Brooks, C. L., III (1999). Development of a Generalized Born model parameterization for proteins and nucleic acids. *J. Phys. Chem. B* **103,** 3765–3773.

Dong, F., Vijayakumar, M., and Zhou, H.-X. (2003). Comparison of calculation and experiment implicates significant electrostatic contributions to the binding stability of barnase and barstar. *Biophys. J.* **85,** 49–60.

Dong, F., and Zhou, H.-X. (2002). Electrostatic contributions to T4 lysozyme stability: Solvent-exposed charges versus semi-buried salt bridges. *Biophys. J.* **83,** 1341–1347.

Draper, D. E., Grilley, D., and Soto, A. M. (2005). Ions and RNA folding. *Annu. Rev. Biophys. Biomol. Struct.* **34,** 221–243.

Dyshlovenko, P. E. (2002). Adaptive numerical method for Poisson–Boltzmann equation and its application. *Comput. Phys. Commun.* **147,** 335–338.

Eisenberg, D., and McLachlan, A. D. (1986). Solvation energy in protein folding and binding. *Nature* **319,** 199–203.

Eisenberg, H. (1976). ''Biological Macromolecules and Polyelectrolytes in Solution,'' Chapter 2. Clarendon, Oxford.

Elcock, A. H., Gabdoulline, R. R., Wade, R. C., and McCammon, J. A. (1999). Computer simulation of protein-protein association kinetics: Acetylcholinesterase-fasciculin. *J. Mol. Biol.* **291,** 149–162.

Elcock, A. H., Potter, M. J., Matthews, D. A., Knighton, D. R., and McCammon, J. A. (1996). Electrostatic channeling in the bifunctional enzyme dihydrofolate reductase-thymidylate synthase. *J. Mol. Biol.* **262,** 370–374.

Elcock, A. H., Sept, D., and McCammon, J. A. (2001). Computer simulation of protein-protein interactions. *J. Phys. Chem. B* **105,** 1504–1518.

Ermak, D. L., and McCammon, J. A. (1978). Brownian dynamics with hydrodynamic interactions. *J. Chem. Phys.* **69,** 1352–1360.

Feig, M., and Brooks, C. L., III (2004). Recent advances in the development and application of implicit solvent models in biomolecule simulations. *Curr. Opin. Struct. Biol.* **14,** 217–224.

Figueirido, F., Delbuono, G. S., and Levy, R. M. (1994). Molecular mechanics and electrostatic effects. *Biophys. Chem.* **51,** 235–241.

Fitch, C. A., Karp, D. A., Lee, K. K., Stites, W. E., Lattman, E. E., and Garcia-Moreno, E. B. (2002). Experimental pKa values of buried residues: Analysis with continuum methods and role of water penetration. *Biophys. J.* **82,** 3289–3304.

Flanagan, M. A., Ackers, G. K., Matthew, J. B., Hanania, G. I. H., and Gurd, F. R. N. (1981). Electrostatic contributions to energetics of dimer-tetramer assembly in human hemoglobin: pH dependence and effect of specifically bound chloride ions. *Biochemistry* **20,** 7439–7449.

Frisch, C., Schreiber, G., Johnson, C. M., and Fersht, A. R. (1997). Thermodynamics of the interaction of barnase and barstar: Changes in free energy versus changes in enthalpy on mutation. *J. Mol. Biol.* **267,** 696–706.

Gabdoulline, R. R., and Wade, R. C. (1997). Simulation of the diffusional association of barnase and barstar. *Biophys. J.* **72,** 1917–1929.

Gabdoulline, R. R., and Wade, R. C. (1998). Brownian dynamics simulation of protein-protein diffusional encounter. *Methods Enzymol.* **14,** 329–341.

Gabdoulline, R. R., and Wade, R. C. (2001). Protein-protein association: Investigation of factors influencing association rates by Brownian dynamics simulations. *J. Mol. Biol.* **306,** 1139–1155.

Gabdoulline, R. R., and Wade, R. C. (2002). Biomolecular diffusional association. *Curr. Opin. Struct. Biol.* **12,** 204–213.

Gallicchio, E., Kubo, M. M., and Levy, R. M. (2000). Enthalpy-entropy and cavity decomposition of alkane hydration free energies: Numerical results and implications for theories of hydrophobic solvation. *J. Phys. Chem. B* **104,** 6271–6285.

Gallicchio, E., and Levy, R. M. (2004). AGBNP: An analytic implicit solvent model suitable for molecular dynamics simulations and high-resolution modeling. *J. Comput. Chem.* **25,** 479–499.

Gallicchio, E., Zhang, L. Y., and Levy, R. M. (2002). The SGB/NP hydration free energy model based on the surface generalized born solvent reaction field and novel nonpolar hydration free energy estimators. *J. Comput. Chem.* **21,** 86–104.

Georgescu, R. E., Alexov, E. G., and Marilyn, R. G. (2002). Combining conformational flexibility and continuum electrostatics for calculating pKas in proteins. *Biophys. J.* **83,** 1731–1748.

Gilson, M. (2000). Introduction to continuum electrostatics. *In* ''Biophysics Textbook Online'' (D. A. Beard, ed.), Biophysical society, Bethesda, MD.

Gilson, M., Davis, M. E., Luty, B. A., and McCammon, J. A. (1993). Computation of electrostatic forces on solvated molecules using the Poisson-Boltzmann equation. *J. Phys. Chem.* **97,** 3591–3600.

Gilson, M. K. (1995). Theory of electrostatic interactions in macromolecules. *Curr. Opin. Struct. Biol.* **5,** 216–223.

Grant, J. A., Pickup, B. T., and Nicholls, A. (2001). A smooth permittivity function for Poisson-Boltzmann solvation methods. *J. Comput. Chem.* **22,** 608–640.

Green, D. F., and Tidor, B. (2005). Design of improved protein inhibitors of HIV-1 cell entry: Optimization of electrostatic interactions at the binding interface. *Proteins* **60,** 644–657.

Hofmeister, F. (1888). Zur lehre von der wirkung der salze. zweite mittheilung. *Arch. Exp. Pathol. Pharmakol.* **24,** 247–260.

Holm, C., Kekicheff, P., and Podgornik, R. (2001). ''Electrostatic Effects in Soft Matter and Biophysics.'' Kluwer academic publishers, Boston, MA.

Holst, M., Baker, N., and Wang, F. (2000). Adaptive multilevel finite element solution of the Poisson-Boltzmann equation i. Algorithms and examples. *J. Comput. Chem.* **21,** 1319–1342.

Holst, M., and Saied, F. (1993). Multigrid solution of the Poisson-Boltzmann equation. *J. Comput. Chem.* **14,** 105–113.

Holst, M. J., and Saied, F. (1995). Numerical solution of nonlinear Poisson-Boltzmann equation: Developing more robust and efficient methods. *J. Comput. Chem.* **16,** 337–364.

Honig, B. H., and Nicholls, A. (1995). Classical electrostatics in biology and chemistry. *Science* **268,** 1144–1149.

Horn, H. W., Swope, W. C., Pitera, J. W., Madura, J. D., Dick, T. J., Hura, G. L., and Head-Gordon, T. (2004). Development of an improved four-site water model for biomolecular simulations: TIP4P-Ew. *J. Chem. Phys.* **120,** 9665–9678.

Humphrey, W., Dalke, A., and Schulten, K. (1996). VMD—visual molecular dynamics. *J. Mol. Graph.* **14,** 33–38.

Ilin, A., Bagheri, B., Scott, L. R., Briggs, J. M., and McCammon, J. A. (1995). Parallelization of Poisson-Boltzmann and Brownian Dynamics calculations. *American Chemical Society Symposium Series* **592,** 170–185.

Im, W., Beglov, D., and Roux, B. (1998). Continuum solvation model: Electrostatic forces from numerical solutions to the Poisson-Boltzmann equation. *Comput. Phys. Commun.* **11,** 59–75.

Irvine, R. F. (2002). Nuclear lipid signaling. *SciSTKE* **150,** 1–12.

Jackson, J. D. (1975). ''Classical Electrodynamics.'' Wiley, New York.

Janin, J., and Chothia, C. (1990). The structure of protein-protein recognition sites. *J. Biol. Chem.* **265,** 16027–16030.

Jensen, J. H., Li, H., Robertson, A. D., and Molina, P. A. (2005). Prediction and rationalization of protein pKa values using QM and QM/MM methods. *J. Phys. Chem. A* **109,** 6634–6643.

Jorgensen, W. L., Chandrasekhar, J., Madura, J. D., Impey, R. W., and Klein, M. L. (1983). Comparison of simple potential functions for simulating liquid water. *J. Chem. Phys.* **79,** 926–935.

Juffer, A. H., Botta, E. F. F., van Keulen, B. A. M., van der Ploeg, A., and Berendsen, H. J. C. (1991). The electric potential of a macromolecule in solvent: A fundamental approach. *J. Comput. Phys.* **97,** 144–171.

Kollman, P. A., Massova, I., Reyes, C., Kuhn, B., Huo, S., Chong, L., Lee, M., Lee, T., Duan, Y., Wang, W., Donini, O., Cieplak, P., *et al.* (2000). Calculating structures and free energies of complex molecules: Combining molecular mechanics and continuum models. *Acc. Chem. Res.* **33,** 889–897.

Krieger, E., Nielsen, J. E., Spronk, C. A. E. M., and Vriend, G. (2006). Fast empirical pKa prediction by Ewald summation. *J. Mol. Graph. Model.* **25**(4), 481–486.

Lamm, G. (2003). The Poisson-Boltzmann Equation. *In* "Reviews in Computational Chemistry" (K. B. Lipkowitz, R. Larter, and T. R. Cundari, eds.), pp. 147–366. John Wiley and Sons, Inc., Hoboken, NJ.

Landau, L. D., Lifshitz, E. M., and Pitaevskii, L. P. (1982). "Electrodynamics of Continuous Media." Butterworth-Heinenann, Boston, MA.

Laux, T., Fukami, K., Thelen, M., Golub, T., Frey, D., and Caroni, P. (2000). GAP43, MARCKS, CAP23 modulate PI(4,5)P2 at plasmalemmal rafts, and regulate cell cortex actin dynamics through a common mechanism. *J. Cell Biol.* **149,** 1455–1472.

Law, M. J., Linde, M. E., Chambers, E. J., Oubridge, C., Katsamba, P. S., Nilsson, L., Haworth, I. S., and Laird-Offringa, I. A. (2006). The role of positively charged amino acids and electrostatic interactions in the complex of U1A protein and U1 hairpin II RNA. *Nucleic Acids Res.* **34,** 275–285.

Leach, A. R. (2001). "Molecular Modeling: Principles and Applications." Prentice Hall, Harlow, England.

Lee, B., and Richards, F. M. (1971). The interpretation of protein structures: Estimation of static accessibility. *J. Mol. Biol.* **55,** 379–400.

Lee, L. P., and Tidor, B. (2001). Optimization of binding electrostatics: Charge complementarity in the barnase-barstar protein complex. *Protein Sci.* **10,** 362–377.

Li, H., Hains, A. W., Everts, J. E., Robertson, A. D., and Jensen, J. H. (2002). The prediction of protein pKa's using QM/MM: The pKa of lysine 55 in turkey ovomucoid third domain. *J. Phys. Chem. B* **106,** 3486–3494.

Li, H., Robertson, A. D., and Jensen, J. H. (2004). The determinants of carboxyl pKa values in turkey ovomucoid third domain. *Proteins* **55,** 689–704.

Lin, J.-H., Baker, N. A., and McCammon, J. A. (2002). Bridging the implicit and explicit solvent approaches for membrance electrostatics. *Biophys. J.* **83,** 1374–1379.

Linderström-Lang, K. (1924). On the ionisation of proteins. *Comptes-rend Lab. Carlaberg* **15,** 1–29.

Livesay, D. R., Jambeck, P., Rojnuckarin, A., and Subramaniam, S. (2003). Conservation of electrostatic properties within enzyme families and superfamilies. *Biochemistry* **42,** 3464–3473.

Lo Conte, L., Chothia, C., and Janin, J. (1999). The atomic structure of protein-protein recognition sites. *J. Mol. Biol.* **285,** 2177–2198.

Luo, R., David, L., and Gilson, M. K. (2002). Accelerated Poisson-Boltzmann calculations for static and dynamic systems. *J. Comput. Chem.* **23,** 1244–1253. http://www3.interscience.wiley.com/cgi-bin/abstract/96516852/ABSTRACT.

Luo, R., Head, M. S., Moult, J., and Gilson, M. K. (1998). pKa shifts in small molecules and HIV protease: Electrostatics and conformation. *J. Am. Chem. Soc.* **120,** 6138–6146.

Luty, B. A., Elamrani, S., and McCammon, J. A. (1993). Simulation of the bimolecular reaction between superoxide and superoxide dismutase—synthesis of the encounter and reaction steps. *J. Am. Chem. Soc.* **115,** 11874–11877.

Ma, B., Elkayam, T., Wolfson, H., and Nussinov, R. (2003). Protein-protein interactions: Structurally conserved residues distinguish between binding sites and exposed protein surfaces. *Proc. Natl. Acad. Sci. USA* **100,** 5772–5777.

MacKerell, A. D., Jr., Bashford, D., Bellot, M., Dunbrack, R. L., Jr., Evanseck, J. D., Field, M. J., Fischer, S., Gao, J., Guo, H., Ha, S., Joseph-McCarthy, D., Kuchnir, L., *et al.* (1998). All-atom empirical potential for molecular modeling and dynamics studies of proteins. *J. Phys. Chem. B* **102,** 3586–3616. http://dx.doi.org/10.1021/jp973084f.

MacKerell, A. D. J., and Nilsson, L. (2001). Nucleic Acid Simulation. *In* "Computational Biochemistry and Biophysics" (O. M. Becker, A. D. J. MacKerell, B. Roux, and M. Watanabe, eds.), pp. 441–463. Marcel Dekker, New York.

Madura, J. D., Briggs, J. M., Wade, R. C., Davis, M. E., Luty, B. A., Antosiewicz, I. J., Gilson, M. K., Bagheri, N., Scott, L. R., and McCammon, J. A. (1995). Electrostatics and diffusion of molecules in solution-simulations with the University of Houston Brownian Dynamics program. *Comput. Phys. Commun.* **91,** 57–95.

Madura, J. D., and McCammon, J. A. (1989). Brownian dynamics simulation of diffusional encounters between triose phosphate isomerase and d-glyceraldehyde phosphate. *J. Phys. Chem.* **93,** 7285–7587.

Manning, G. S. (1978). The molecular theory of polyelectrolyte solutions with applications to the electrostatic properties of polynucleotides. *Q. Rev. Biophys.* **11,** 179–246.

Martin, T. F. (2001). PI(4,5)P2 regulation of surface membrane traffic. *Curr. Opin. Cell Biol.* **13,** 493–499.

Massova, I., and Kollman, P. A. (2000). Combined molecular mechanical and continuum solvent approach (MM-PBSA/GBSA) to predict ligand binding. *Perspect. Drug Discovery Des.* **18,** 113–135.

Masunov, A., and Lazaridis, T. (2003). Potentials of mean force between ionizable aminoacid side-chains in aqueous solution. *J. Am. Chem. Soc.* **125,** 1722–1730.

McLaughlin, S., Wang, J., Gambhir, A., and Murray, D. (2002). PIP2 and proteins: Interactions, organization and information flow. *Annu. Rev. Biophys. Biomol. Struct.* **31,** 151–175.

McQuarrie, D. A. (2000). ''Statistical Mechanics.'' University Science Books, Sausalito, CA.

Micu, A. M., Bagheri, B., Ilin, A. V., Scott, L. R., and Pettitt, B. M. (1997). Numerical considerations in the computation of the electrostatic free energy of interaction within the poisson-boltzmann theory. *J. Comput. Phys.* **136,** 263–271.

Misra, V. K., and Draper, D. E. (2000). Mg(2+) binding to tRNA revisited: The nonlinear Poisson-Boltzmann model. *J. Mol. Biol.* **299,** 1135–1147.

Misra, V. K., and Draper, D. E. (2001). A thermodynamic framework for Mg^{2+} binding to RNA. *Proc. Natl. Acad. Sci. USA* **98,** 12456–12461.

Misra, V. K., Hecht, J. L., Yang, A.-S, and Honig, B. (1998). Electrostatic contributions to the binding free energy of λcI repressor to DNA. *Biophys. J.* **75,** 2262–2273.

Moore, K. J. M., and Lohman, T. M. (1994). Kinetic mechanism of adenine nucleotide binding to and hydrolysis by the *Escherichia coli* Rep monomer. 2. Application of a kinetic competition approach. *Biochemistry* **33,** 14565–78.

Mueller, U., Perl, D., Schmid, F. X., and Heinemann, U. (2000). Thermal stability and atomic-resolution crystal structure of the *Bacillus caldolyticus* cold shock protein. *J. Mol. Biol.* **297,** 975–988.

Murray, D., Ben-Tal, N., Honig, B., and McLaughlin, S. (1997). Electrostatic interaction of myristoylated proteins with membranes: Simple physics, complicated biology. *Structure* **5,** 985–989.

Nicholls, A., and Honig, B. (1991). A rapid finit difference algorithm, utilizing successive over-relaxation to solve the Poisson-Boltamann equation. *J. Comput. Chem.* **12,** 435–445.

Nielsen, J. E., and McCammon, J. A. (2003). On the evaluation and optimization of protein x-ray structures for pKa calculations. *Protein Sci.* **12,** 313–326.

Nielsen, J. E., and Vriend, G. (2001). Optimizing the hydrogen-bond network in poisson-boltzmann equation-based pk(a) calculations. *Proteins* **43,** 403–412.

Nonner, W., Gillespe, D., Henderson, D., and Eisenberg, D. (2001). Ion accumulation in biologycal calcium channel: Effects of solvent and confining pressure. *J. Phys. Chem. B* **105,** 6427–6436.

Norel, R., Sheinerman, F., Petrey, D., and Honig, B. (2001). Electrostatic contributions to protein-protein interactions: Fast energetic filters for docking and their physical basis. *Protein Sci.* **10,** 2147–2161.

Northrup, S. H., Allison, S. A., and McCammon, J. A. (1984). Brownian dynamics simulation of diffusion-influenced biomolecular reactions. *J. Chem. Phys.* **80,** 1517–1524.

Novotny, J., and Sharp, K. (1992). Electrostatic fields in antibodies and antibody/antigen complexes. *Prog. Biophys. Mol. Biol.* **58,** 203–224.

Onufriev, A., Case, D. A., and Bashford, D. (2002). Effective born radii in the Generalized Born approximation: The importance of being perfect. *J. Comput. Chem.* **23,** 1297–1304.

Osapay, K., Young, W. S., Bashford, D., Brooks, C. L., III, and Case, D. A. (1996). Dielectric continuum models for hydration effects on peptide conformation transitions. *J. Phys. Chem.* **100,** 2698–2705.

Overman, L. B., and Lohman, T. M. (1994). Lingkage of pH, aion and cation effectx in protein-nucleic acid equilibria. *Escherichia coli* SSB protein-single strand nucleic acid interactions. *J. Mol. Biol.* **236,** 165–178.

Pace, C. N. (2000). Single surface stabilizer. *Nat. Struct. Biol.* **7,** 345–346.

Payrastre, B., Missy, K., Giuriato, S., Bodin, S., Plantavid, M., and Gratacap, M. (2001). Phosphoinositides: Key players in cell signalling, in time and space. *Cell. Signal.* **13,** 377–387.

Perl, D., Mueller, U., Heinemann, U., and Schmid, F. X. (2000). Two exposed amino acid residues confer thermostability on a cold shock protein. *Nat. Struct. Biol.* **7,** 380–383.

Perl, D., and Schmid, F. X. (2001). Electrostatic stabilization of a thermophilic cold shock protein. *J. Mol. Biol.* **213,** 343–357.

Ponder, J. W., and Case, D. A. (2003). Force fields for protein simulations. *Adv. Protein Chem.* **66,** 27–85.

Radic, Z., Kirchhoff, P. D., Quinn, D. M., McCammon, J. A., and Taylor, P. (1997). Electrostatic influence on the kinetics of ligand binding to acetylcholinesterase. *J. Biol. Chem.* **272,** 23265–23277.

Rauch, M. E., Ferguson, C. G., Prestwich, G. D., and Cafiso, D. (2002). Myristoylated alanine-rich C kinase substrate (MARCKS) sequesters spin-labeled phosphatidylinositol-4,5-bisphosphate in lipid bilayers. *J. Biol. Chem.* **277,** 14068–14076.

Raucher, D., Stauffer, T., Chen, W., Shen, K., Guo, S., York, J. D., Sheetz, M. P., and Meyer, T. (2000). Phosphatidylinositol 4,5-bisphosphate functions as a second messenger that regulates cytoskeleton-plasma membrane adhesion. *Cell* **100,** 221–228.

Record, M. T., Ha, J.-H., and Fisher, M. A. (1991). Analysis of equilibrium and kinetic measurements to determine thermodynamic origins of stability and specificity and mechanism of formation of site-specific complexes between proteins and helical DNA. *Methods Enzymol.* **208,** 291–343.

Reuter, H., Pott, C., Goldhaber, J. I., Henderson, S. A., Philipson, K. D., and Schwinger, R. H. (2005). Na(+)—Ca^{2+} exchange in the regulation of cardiac excitation-contraction coupling. *Cardiovasc Res.* **67,** 198–207.

Rocchia, W., Alexov, E., and Honig, B. (2001). Extending the applicability of the nonlinear Poisson-Boltzmann equation: Multiple dielectric constants and multivalent lons. *J. Phys. Chem. B* **105**(28), 6507–6514.

Römer, R., and Hach, R. (1975). tRNA conformation and magnesium binding. A study of a yeast phenylalanine-specific tRNA by a fluorescent indicator and differential melting curves. *Eur. J. Biochem.* **55,** 271–284.

Romer, R., and Hach, R. (1975). tRNA conformation and magnesium binding. A study of yeast phenylalanine-specific tRNA by fluorecent indicator and differential melting curves. *Eur. J. Biochem.* **55,** 271–284.

Roux, B. (2001). Implicit solvent models. *In* "Computational Biochemistry and Biophysics" (O. M Becker, A. D. Mackerell, Jr., B. Roux, and M. Watanabe, eds.), pp. 133–152. Marcel Dekker, New York.

Roux, B., and Simonson, T. (1999). Implicit solvent models. *Biophys. Chem.* **78,** 1–20.

Russell, R. B., Alber, F., Aloy, P., Davis, F. P., Korkin, D., Pichaud, M., Topf, M., and Sali, A. (2004). A structural perspective on protein-protein interactions. *Curr. Opin. Struct. Biol.* **14,** 313–324.

Sagui, C., and Darden, T. A. (1999). Molecular dynamics simulation of biomolecules: Long-range electrostatic effects. *Annu. Rev. Biophys. Biomol. Struct.* **28,** 155–179.

Schaeler, M., and Karplus, M. (1996). A comprehensive analytical treatment of continuum electrostatics. *J. Phys. Chem.* **100,** 1578–1599.

Schlick, T. (2002). "Molecular Modeling and Simulation: An Interdisciplinary Guide." Springer-Verlag, New York.

Schreiber, G., and Fersht, A. R. (1993). Interaction of barnase with its polypeptide inhibitor barstar studied by protein engineering. *Biochemistry* **32,** 5145–5150.

Schreiber, G., and Fersht, A. R. (1995). Energetics of protein-protein interactions: Analysis of the barnase-barstar interface by single mutations and double mutant cycles. *J. Mol. Biol.* **248,** 478–486.

Senear, D. F., and Batey, R. (1991). Comparison of operator-specific and nonspecific interactions of lambda cI repressor: [KCL] and pH effects. *Biochemistry* **30,** 6677–6688.

Sept, D., Baker, N. A., and McCammon, J. A. (2003). The physical basis of microtubule structure and stability. *Protein Sci.* **12,** 2257–2261.

Sept, D., Elcock, A. H., and McCammon, J. A. (1999). Computer simulations of actin polymerization can explain the barbed-pointed end asymmetry. *J. Mol. Biol.* **294,** 1181–1189.

Sept, D., and McCammon, J. A. (2001). Thermodynamics and kinetics of actin filament nucleation. *Biophys. J.* **81,** 667–674.

Sharp, K. A., and Honig, B. H. (1990). Electrostatic interactions in macromolecules: Theory and applications. *Annu. Rev. Biophys. Biophys. Chem.* **19,** 301–332.

Sharp, K. A., Nicholls, A., Fine, R. F., and Honig, B. (1991). Reconciling the magnitude of the microscopic and macroscopic hydrophobic effects. *Science* **252,** 106–109.

Sheinerman, F. B., and Honig, B. (2002). On the role of electrostatic interactions in the design of protein-protein interfaces. *J. Mol. Biol.* **318,** 161–177.

Sheinerman, F. B., Norel, R., and Honig, B. (2000). Electrostatic aspects of protein-protein interactions. *Curr. Opin. Struct. Biol.* **10,** 153–159.

Shimizu, S. (2004). Estimating hydration changes upon biomolecular reactions from osmotic stress, high pressure, and preferential hydration experiments. *Proc. Natl. Acad. Sci. USA* **101,** 1195–1199.

Shimizu, S., and Smith, D. (2004). Preferential hydration and the exclusion of cosolvents from protein surfaces. *J. Chem. Phys.* **121,** 1148–1154.

Simonson, T. (2003). Electrostatics and dynamics of proteins. *Rep. Prog. Phys.* **66,** 737–787.

Simonson, T., and Brunger, A. T. (1994). Solvation free energies estimated from macroscopic continuum theory: An accuracy assessment. *J. Phys. Chem.* **98,** 4683–4694.

Sines, J. J., McCammon, J. A., and Allison, S. A. (1992). Kinetic effects of multiple charge modifications in enzyme-substrate reactions—Brownian Dynamics simulations of Cu, Zn superoxide dismutase. *J. Comput. Chem.* **13,** 66–69.

Sitkoff, D., Sharp, K. A., and Honig, B. (1994a). Correlating solvation free energies and surface tensions of hydrocarbon solutes. *Biophys. Chem.* **51,** 397–409.

Sitkoff, D., Sharp, K. A., and Honig, B. H. (1994b). Accurate calculation of hydration free energies using macroscopic solvent models. *J. Phys. Chem.* **98,** 1978–1988.

Spaar, A., Dammer, C., Gabdoulline, R. R., Wade, R. C., and Helms, V. (2006). Diffusional encounter of barnase and barstar. *Biophys. J.* **90,** 1913–1924.

Spaar, A., and Helms, V. (2005). Free energy landscape of protein-protein encounter resulting from brownian dynamics simulations of barnase:Barstar. *J. Chem. Theory Comput.* **1,** 723–736.

Spolar, R. S., Ha, J. H., and Record, M. T. J. (1989). Hydrophobic effect in protein folding and other noncovalent processes involving proteins. *Proc. Natl. Acad. Sci. USA* **86,** 8382–8385.

Stein, A., and Crothers, D. M. (1976). Conformational changes of transfer RNA. The role of magnesium(II). *Biochemistry* **15,** 160–167.

Still, W. C., Tempczyk, A., Hawley, R. C., and Hendrickson, T. (1990). Semianalytical treatment of solvation for molecular mechanics and dynamics. *J. Am. Chem. Soc.* **112,** 6127–6129.

Su, Y., and Gallicchio, E. (2004). The non-polar solvent potential of mean force for the dimerization of alanine dipeptide: The role of solute-solvent van der Waals interactions. *Biophys. Chem.* **109,** 251–260.

Swanson, J. M. J., Henchman, R. H., and McCammon, J. A. (2004). Revisiting free energy calculations: A theoretical connection to MM/PBSA and direct calculation of the association free energy. *Biophys. J.* **86,** 67–74.

Tan, R. C., Truong, T. N., McCammon, J. A., and Sussman, J. L. (1993). Acetylcholinesterase—electrostatic steering increases the rate of ligand binding. *Biochemistry* **32,** 401–403.

Tanford, C., and Kirkwood, J. G. (1957). Theory of protein titration curves. I. General equations for impenetrable spheres. *J. Am. Chem. Soc.* **79,** 5333–5339.

Tanford, C., and Roxby, R. (1972). Interpretation of protein titration curves. *Biochemistry* **11,** 2192–2198.

Tara, S., Elcock, A. H., Kirchhoff, P. D., Briggs, J. M., Radic, Z., Taylor, P., and McCammon, J. A. (1998). Rapid binding of a cationic active site inhibitor to wild type and mutant mouse acetylcholinesterase: Brownian dynamics simulation including diffusion in the active site gorge. *Biopolymers* **46,** 465–474.

Toker, A. (1998). The synthesis and cellular roles of phosphatidylinositol 4,5-bisphosphate. *Curr. Opin. Cell Biol.* **10,** 254–261.

Vasker, I. A. (2004). Protein-protein interfaces are special. *Structure* **12,** 910–912.

Verwey, E. J. W., and Overbeek, J. T. G. (1999). ''Theory of Stability of Lyophobic Colloids.'' Dover Publications, Inc., Mineola, New York.

Wagoner, J., and Baker, N. A. (2004). Solvation forces on biomolecular structures: A comparison of explicit solvent and Poisson-Boltzmann models. *J. Comput. Chem.* **25,** 1623–1629.

Wagoner, J. A., and Baker, N. A. (2006). Assessing implicit models for nonpolar mean solvation forces: The importance of dispersion and volume terms. *Proc. Natl. Acad. Sci. USA* **103,** 8331–8336.

Wang, J., Arbuzova, A., Hangyas-Mihalyne, G., and McLaughlin, S. (2001a). The effector domain of myristoylated alanine-rich C kinase substrate (MARCKS) binds strongly to phosphatidylinositol 4,5-bisphosphate (PIP2). *J. Biol. Chem.* **276,** 5012–5019.

Wang, J., Gambhir, A., Hangyas-Mihalyne, G., Murray, D., Golebiewska, U., and McLaughlin, S. (2002). Lateral sequestration of phosphatidylinositol 4,5-bisphosphate by the basic effector domain of myristoylated alanine-rich C kinase substrate is due to nonspecific electrostatic interactions. *J. Biol. Chem.* **277,** 34401–34412.

Wang, J., Gambhir, A., McLaughlin, S., and Murray, D. (2004). A computational model for the electrostatic sequestration of PI(4,5)P2 by membrane-adsorbed basic peptides. *Biophys. J.* **86,** 1969–1986.

Wang, T., and Wade, R. C. (2003). Implicit solvent models for flexible protein-protein docking by molecular dynamics simulation. *Proteins* **50,** 158–169.

Wang, W., Donini, O., Reyes, C. M., and Kollman, P. A. (2001b). Biomolecular simulations: Recent development in force fields, simulationa of enzyme catalysis, protein-ligand, protein-protein, and protein-nucleic acid noncovalent interactions. *Annu. Rev. Biophys. Biomol. Struct.* **30,** 211–243.

Warwicker, J., and Watson, H. C. (1982). Calculation of the electric potential in the active site cleft due to alphs-helix dipoles. *J. Mol. Biol.* **157,** 671–679.

Wesson, L., and Eisenberg, D. (1992). Atomic solvation parameters applied to molecular dynamics of proteins in solution. *Protein Sci.* **1,** 227–235.

Wong, C. F., Hünenberger, P. H., Akamine, P., Narayana, N., Diller, T., McCammon, J. A., Taylor, S., and Xuong, N.-H. (2001). Computational analysis of PKA-balanol interactions. *J. Med. Chem.* **44,** 1530–1539.

Xu, D., Lin, S. L., and Nussinov, R. (1997). Protein binding versus protein folding: The role of hydrophilic bridges in protein associations. *J. Mol. Biol.* **265,** 68–84.

Yin, H. L., and Janmey, P. A. (2003). Phosphoinositide regulation of the actin cytoskeleton. *Annu. Rev. Physiol.* **65,** 761–789.

Yu, Z., Jacobson, M. P., Josovitz, J., Rapp, C. S., and Friesner, R. A. (2004). First-shell solvation of ion pairs: Correction of systematic errors in implicit solvent models. *J. Phys. Chem. B* **108,** 6643–6654.

Zauhar, R. J., and Morgan, R. J. (1988). The rigorous computation of the molecular electric potential. *J. Comput. Chem.* **9,** 171–187.

Zhou, H. X. (2005). Interactions of macromolecules with salt ions: An electrostatic theory for the Hofmeister effect. *Proteins* **61,** 69–78.

Zhou, H. X., and Dong, F. (2003). Electrostatic contributions to the stability of a thermophilic cold shock protein. *Biophys. J.* **84,** 2216–2222.

Zhu, Z. Y., and Karlin, S. (1996). Clusters of charged residues in protein three-dimensional structures. *Proc. Natl. Acad. Sci. USA* **93,** 8350–8355.